

# Object-based land-use/land-cover change detection using Landsat imagery: a case study of Ardabil, Namin, and Nir counties in northwest Iran

Farnoosh Aslami · Ardavan Ghorbani

Received: 27 December 2017 / Accepted: 25 May 2018 / Published online: 3 June 2018  
© Springer International Publishing AG, part of Springer Nature 2018

**Abstract** In this study, land-use/land-cover (LULC) change in the Ardabil, Namin, and Nir counties, in the Ardabil province in the northwest of Iran, was detected using an object-based method. Landsat images including Thematic Mapper (TM), Landsat Enhanced Thematic Mapper Plus (ETM<sup>+</sup>), and Operational Land Imager (OLI) were used. Preprocessing methods, including geometric and radiometric correction, and topographic normalization were performed. Image processing was conducted according to object-based image analysis using the nearest neighbor algorithm. An accuracy assessment was conducted using overall accuracy and Kappa statistics. Results show that maps obtained from images for 1987, 2002, and 2013 had an overall accuracy of 91.76, 91.06, and 93.00%, and a Kappa coefficient of 0.90, 0.83, and 0.91, respectively. Change detection between 1987 and 2013 shows that most of the rangelands (97,156.6 ha) have been converted to dry farming; moreover, residential and other urban land uses have also increased. The largest change in land use has occurred for irrigated farming, rangelands, and dry farming, of which approximately 3539.8, 3086.9, and

2271.9 ha, respectively, have given way to urban land use for each of the studied years.

**Keywords** Remote sensing · Land use/land cover · Change detection · Object-based image analysis · Landsat · Ardabil province

## Introduction

Remote sensing provides a broad view of landscapes and consistent record through time, making it an important tool for monitoring and managing land resources (Phinn et al. 2002). Change detection is the process of identifying differences in the state of an object or phenomenon by observing it at different times (Coppin et al. 2004). Accurate change detection of land use/land cover (LULC) has become a key issue for monitoring local, regional, and global environments and resources, providing the foundation for a better understanding of relationships and interactions between humans and natural phenomena in order to improve management and use of resources (Lu et al. 2004). Remote sensing has been used as a powerful tool in change detection applications and provides cost-effective multi-temporal satellite images. Since the early 1970s, these data, along with remote sensing analytical approaches, have been of considerable interest for periodic monitoring of large LULC in natural and built environments (Phinn et al. 2002; Griffiths et al. 2010; Jayanth et al. 2016). Considering the importance of remote sensing in evaluating changes

---

F. Aslami  
Department of Natural Geography, Faculty of Humanities,  
University of Mohaghegh Ardabili, Ardabil, Iran  
e-mail: Farnoosh.aslami@yahoo.com

A. Ghorbani (✉)  
Department of Natural Resources, Faculty of Agricultural  
Technology and Natural Resources, University of Mohaghegh  
Ardabili, Ardabil 5619911367, Iran  
e-mail: a\_ghorbani@uma.ac.ir

in landscape cover, this technique was selected for the present study. A popular and commonly used approach for image analysis is digital image classification. The purpose of image classification is to label the pixels in the image with meaningful information from the real world. Through classification of digital remote sensing images, thematic maps bearing information such as land-cover type and vegetation type can be obtained. Subsequently, change detection may be carried out based on these thematic maps (Dewan and Yamaguchi 2009; El-Asmar et al. 2013; Rawat and Kumar 2015; Ghebregabher et al. 2016). Traditionally, pixel-based techniques usually were used to create LULC classifications (Erbek et al. 2004; Weih and Riggan 2010; Taati et al. 2015). The pixel-based techniques include either a supervised or unsupervised classification or a combination of these (Enderle and Weih 2005; Weih and Riggan 2010). These methods only analyze the pixels' spectral signatures without any consideration to the spatial or contextual information of each pixel. eCognition® software package has been developed utilizing object-based classification. The package uses a segmentation process and learning algorithm to analyze both the spectral and spatial/contextual properties of pixels procedures (Weih and Riggan 2010). This process provides a semi-automatic classification that could be more accurate than traditional pixel-based methods (Weih and Riggan 2010; Whiteside et al. 2011; Jawak et al. 2015; Butt et al. 2015; Sinha et al. 2015). There is increasing attention on object-based classification (Du et al. 2013; Long et al. 2013; Im et al. 2013; Aslami et al. 2015; Hussain and Shan 2015), which has already been reviewed by Blaschke (2010). Moreover, an ArcGIS Python model was developed by Wells (2010) utilizing polygon extraction from aerial images and producing land-cover map. As for the advantages of object-based classification comparing with pixel-based methods, we can briefly mention (1) higher potential for processing high-volume data in lower time since it uses segments (a group of similar pixels) not individual pixels; (2) utilizing segments or objects representing characteristic texture features which are ignored in traditional methods; (3) doing the classification in two steps (segmentation and classification) providing the chance of obtaining the higher accuracy due to applying all spectral, textural and contextual information in the same time for classification (Gao and Mas 2008), and (4) eCognition package provides a more user-

friendly environment for experts in all steps of classification and post-classification. This technique is considered in this study due to its success in several research using Landsat images, such as Lewinski (2006), Al Fugara et al. (2009), Roostaie et al. (2012), Amalimana et al. (2017) and Phiri and Mogenroth (2017).

Myint et al. (2011) used a QuickBird image over a central region in the city of Phoenix for object-based classification. They selected 0.1 and 0.5 for the shape and compactness factors, respectively, and selected 10 different objects per class at scales of 10, 25, 50, and 100 to perform a discriminant analysis for segmentation, finally settling on a scale of 100 for their study. They then classified the image using a nearest neighbor classifier with an accuracy of 90.40%. There are some other studies using Landsat series, the appropriate accuracy assessment criteria (Campbell et al. 2015), and several segmentation parameters which obtained higher overall accuracy, including Li et al. (2015), Olmanson and Bauer (2016), and Cheţan et al. (2017).

Over the study area, the traditional land management and land-use planning with rapid population growth particularly during recent decades resulted in unrestrained settlement/industrial/ recreational areas in addition to agricultural land expansion which pose crucial challenges for environment managers in various aspects especially in Ardabil County with a traditional economy. Attentive monitoring at fine temporal/spatial scales would reveal a fluctuating landscape, punctuated by changes in movement of people, perturbation from environmental disasters, and shifts in activities. On the other hand, the lack of financial support to scientific research have made researchers in Iran to find and evaluate the free, relatively high spatial/temporal remotely sensed data for land and environment monitoring (Akbari et al. 2007; Solaimani et al. 2010; Amini Parsa and Salehi 2016; Halimi et al. 2017; Mirzaei et al. 2018). Thus, the applied, using free satellite images and new cost-effective processing techniques and resulted information, can enable regional/local planners as well as policy makers to identify and manage LULC changes better. Moreover, the methodology can be evaluated by other researchers in other regions for similar aims.

Already, we have compared Artificial Neural Network (ANN), Support Vector Machine (SVM), and Maximum Likelihood (ML) methods with object-based classification technique for the preparation of

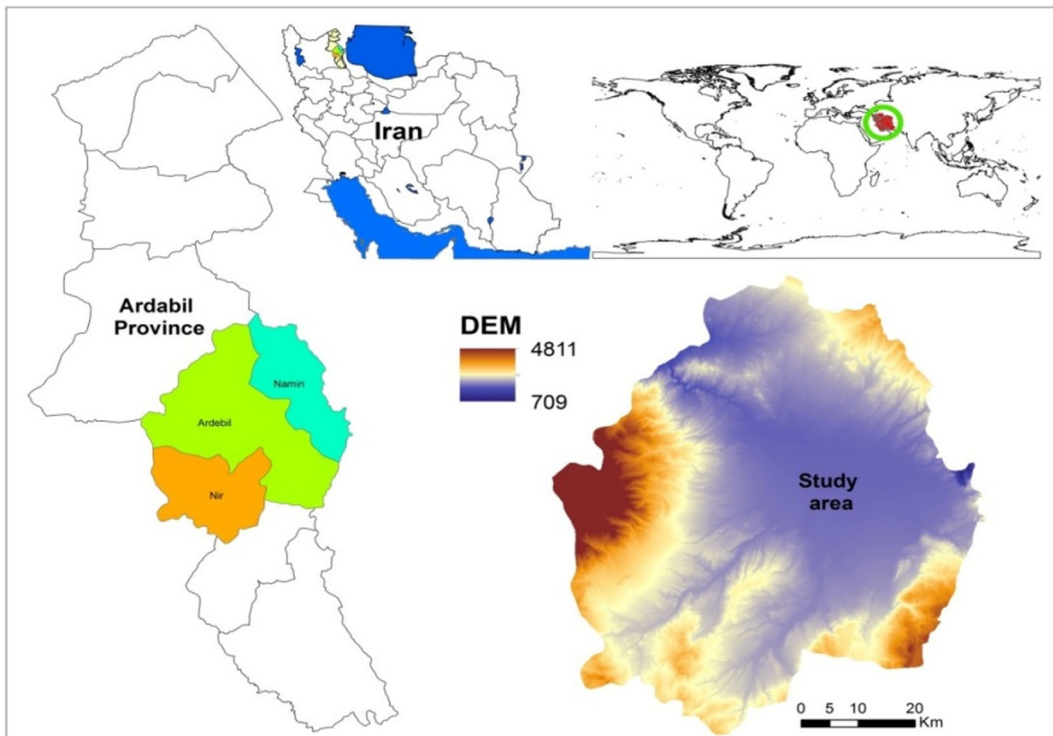


**Fig. 1** Digital elevation model (DEM) of the study area (Ardabil, Namin, and Nir counties) in Ardabil province, Iran, and the world, with topographic variation

LULC map using Landsat-8 images in Ardabil, Namin, and Nir counties, in the Ardabil province in the northwest of Iran, and concluded that the object-based technique provided with more reliable results in comparison (Aslami et al. 2015), following in this study we have conducted to detect LULC changes in the study area using object-based image analysis and Landsat data.

**Materials and methods**

**Study area**

The study area is located at 47° 46' to 48° 42' E and 37°48' to 38° 38' N (Fig. 1), covering an area of 4726 km<sup>2</sup>. The Ardabil plain is situated at the center of the study area, with agriculture as its primary land use

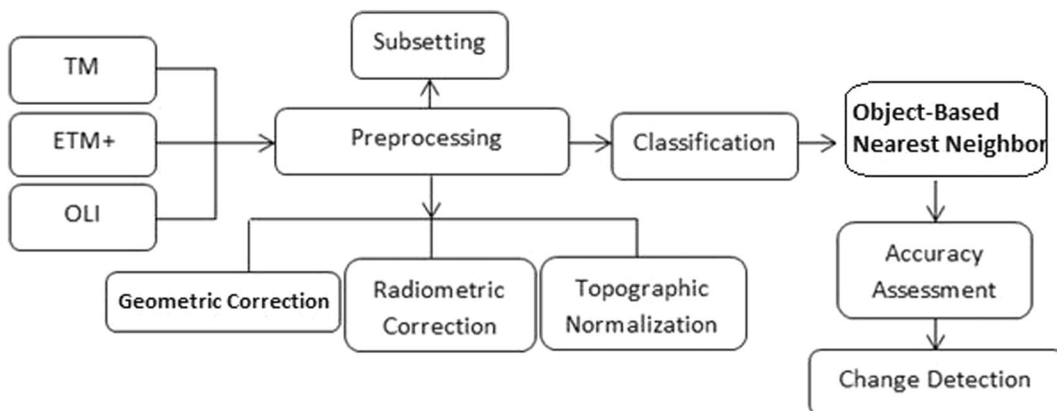


**Fig. 2** The framework of the employed principal procedure

**Table 1** Characteristics of the selected images

Landsat sensor	Imagery date	Row/path	Sun azimuth	Sun elevation	Number of used bands	Spatial resolution
TM	1987/06/10	167/33	115.48	61.47	6	30 m
	1987/09/30	167/34	143.42	44.00		
ETM <sup>+</sup>	2002/07/29	167/33	125.69	60.63	6	
		167/34	123.09	61.23		
OLI	2013/07/19	167/33	128.21	64.36	8	
		167/34	125.25	64.99		

(mainly potato and wheat cultivation) in addition to residential and industrial areas. Mount Sabalan is the third highest summit in Iran with a height of 4811 m above sea level and is situated in the west of the study area, which is dominated by rangeland (shrubland, grass-shrublands, grasslands, and approximately 32 wetlands); it serves the Shahsavani nomads as their summer rangeland (Sharifi et al. 2013; Ghorbani et al. 2018). Highlands at the south and northeast are also primarily rangeland (mainly shrub-grasslands). Areas of low altitude in the east are covered by scattered forest, which is dominated by Euro-Siberian species such as *Quercus castaneifolia*, *Quercus macranthera*, *Fagus orientalis*, *Corylus avellana*, and *Acer campestre* (Teimoorzadeh et al. 2015). Since 1993, when new country political divisions have made the area and some other surrounding counties as a new province (Ardabil province, which has separated from East Azerbaijan province), population concentration has been increased in the study area as the capital city of Ardabil province; consequently, new industrial, commercial, and recreational sets have been developed. Moreover, due to the new policy for tourists' attractions in the province, more than 6 million tourists dominantly not respecting the natural environment annually visit the area. Their need for more cross-road service complexes and ski resorts on one hand and development of Sarien city due to its

different spa facilities on the other hand have made the situation even worse because of building lots of restaurants and shopping centers in different natural areas. All these resulted in expanding border cities (Ardabil, Namin, Nir, Sarien, Hir, Abibagloo, and Samian) and their population needing more land for agriculture, cultivating rangeland mainly for planting irrigated/rainfed wheat, barley, and potatoes, and building farmland (mainly irrigated farms) (Ghorbani et al. 2011). The elevation of the study area ranges from 709 to 4811 m and experiences harsh winters and moderately cool summers with average annual temperatures ranging from  $-3$  to  $13$  °C, and annual precipitation from 215 to 766 mm.

The overall framework of the study is presented in Fig. 2.

#### Image selection

The seasonality and phenological patterns (Reed et al. 2003) of the study area were considered, according to observations at an altitude of 4102 m, and no considerable seasonal variation was found. However, phenological stages were found to be different, with four discernible seasons, in addition to different temperatures, and types and amounts of precipitation at different elevations. It was thus decided that the best time of the year

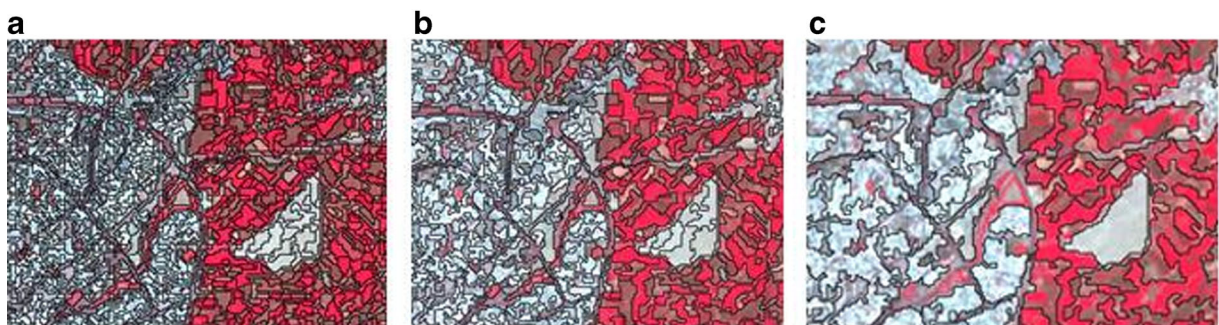


**Fig. 3** Results of three segmentations using different scale values for part of the study area. **a** 30. **b** 60. **c** 130



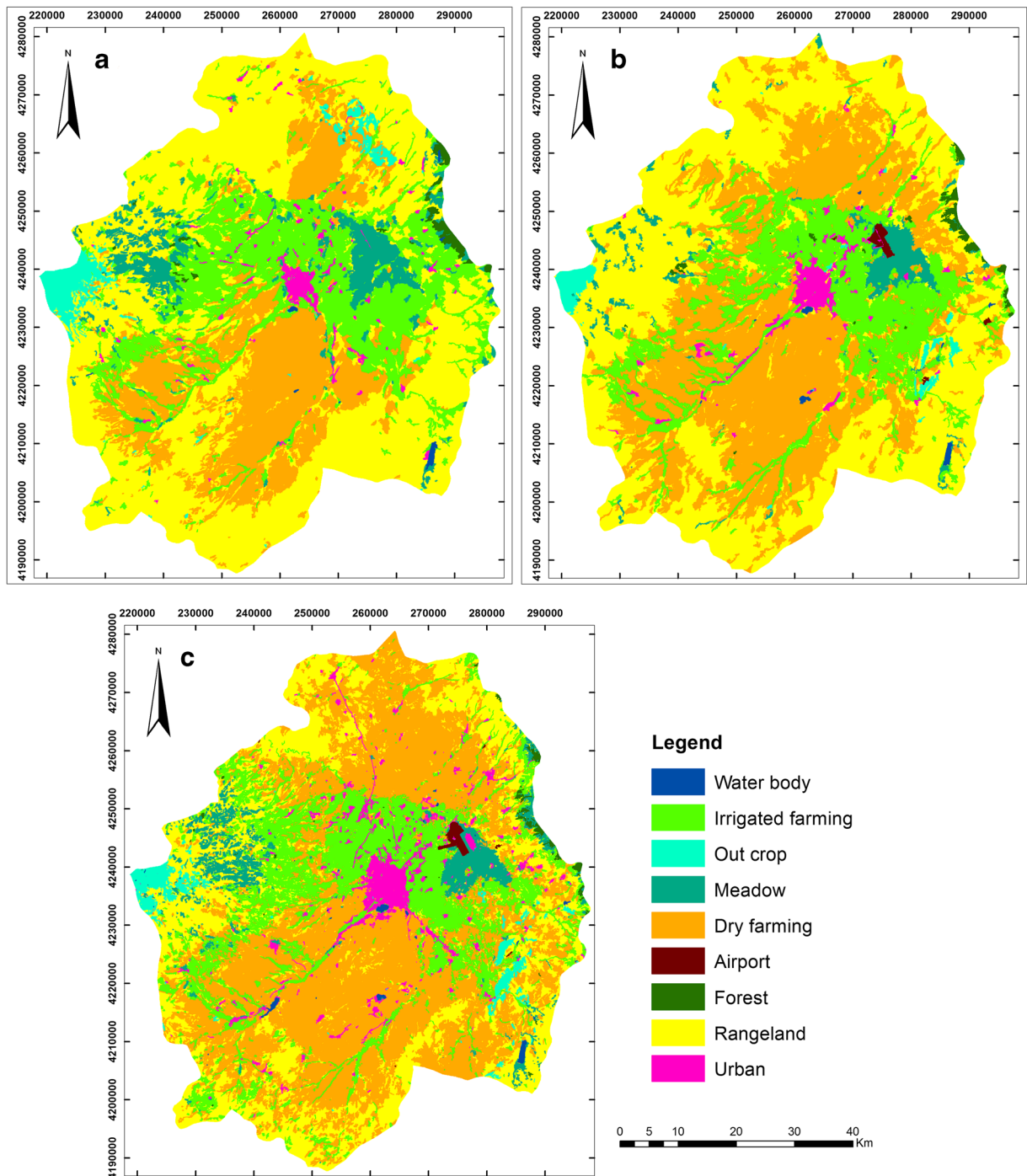


**Fig. 4** Land use maps of **a** 1987, **b** 2002, and **c** 2013 for the study area produced using the object-based method

for images was late April to early May. In the case that moisture would affect the data acquired from these images, dates 15 days earlier were also considered; however, there was no noticeable precipitation during

this period. Finally, images including Landsat Thematic Mapper (TM), Enhanced Thematic Mapper Plus (ETM<sup>+</sup>), and Operational Land Imager (OLI) were selected (Table 1).

**Table 2** Summary of accuracy assessment

Maps	1987	2002	2013
Overall accuracy (%)	91.76	91.06	93.00
Kappa	0.90	0.83	0.91

Image preprocessing

Preprocessing is critical in change detection studies because it is assumed that the spectral properties of non-changed areas remain stable, and inadequate preprocessing can increase the potential for error by causing detection of false change in the spectral space (Lu et al. 2004; Wulder et al. 2006).

Initially, a digital elevation model (DEM) map of the study area was produced (the DEM was extracted using 1:25000 topographic maps of National Cartographic Center of Iran, with 10 m horizontal and vertical accuracy) using ArcGIS10 (Fig. 1). The image preprocessing stages, including geometric correction, radiometric controlling, topographic normalization, and image enhancement, were conducted before image processing (Chander and Markham 2003; Lillesand et al. 2008). The obtained image was registered to the UTM projection with the WGS84 datum. However, according to the collected 16 ground control points (GCPs) using Garmin Oregon 550 GPS and some geographical information systems (GIS) layers such as registered topographic map, the acquired images still required rectification. The affine transformation model which is widely used for

**Table 3** Areas of land-use types

Land use	Area (ha)			
	ID	1987	2002	2013
Water body	1	634.20	719.08	958.21
Irrigated farming	2	90,105.49	70,209.35	80,567.08
Outcrop	3	9914.73	4594.74	7123.51
Meadow	4	11,048.14	9666.91	6507.58
Dry farming	5	100,623.72	163,000.87	208,671.01
Forest	6	10,295.27	2687.82	3344.03
Rangeland	7	244,522.75	214,074.34	150,918.24
Urban	8	5424.37	6685.55	13,314.48
Airport	9	0.00	1130.67	1166.15

geometric corrections was used to geometrically correct the images to align accurately with the collected GPS points. Therefore, images were geometrically corrected (UTM/WGS84), and then controlled using 16 known GCPs (crossroads). According to the concept of change detection, radiometric correction is a necessary step in image preprocessing. For radiometric correction, the following equations, taken from the official Landsat site, were used for the three selected images. Equation 1 was used for the TM image and Eq. 2 for the ETM+ image to convert the digital number (DN) to radiance:

$$L_{\lambda} = Gain \times QCAL + Bias \tag{1}$$

$$L_{\lambda} = ((Lmax_{\lambda} - Lmin_{\lambda}) / (QCALmax - QCALmin)) \times (QCAL - QCALmin) + Lmin_{\lambda} \tag{2}$$

where *Gain* is rescaled gain (m<sup>2</sup>\*ster\*µm), *Bias* is rescaled bias (m<sup>2</sup>\*ster\*µm), *QCAL* is the quantified calibrated pixel value (DN), *L<sub>λ</sub>* is the spectral radiance of the sensor’s aperture in watts/(m<sup>2</sup>\*ster\*µm), *Lmin<sub>λ</sub>* is the spectral radiance scaled to *QCALmin* in watts/(m<sup>2</sup>\*ster\*µm), *Lmax<sub>λ</sub>* is the spectral radiance scaled to *QCALmax* in watts/(m<sup>2</sup>\*ster\*µm), *QCALmin* is the minimum quantized pixel value in DN, and *QCALmax* is the maximum quantized pixel value in DN. Equation 3 was used to convert radiance to Top of Atmosphere (TOA) reflectance for TM and ETM+ sensors:

$$\rho_p = \frac{\pi \cdot L_{\lambda} \cdot d^2}{ESUN_{\lambda} \cdot \cos\theta_s} \tag{3}$$

where  $\rho_p$  is unit less TOA or planetary reflectance, *d* is earth-sun distance in astronomical units, *ESUN<sub>λ</sub>* is the mean solar exoatmospheric spectral irradiance, and  $\theta_s$  is the solar zenith angle in degrees. OLI images were corrected using Eq. 4, which directly converts DN to TOA reflectance:

$$\lambda\rho = \frac{M_{\rho} Q_{cal} + A_{\rho}}{\sin(\theta_{SE})} \tag{4}$$

where *M<sub>ρ</sub>* is multiplicative rescaling factor, *A<sub>ρ</sub>* is additive rescaling factor, which both are band-specific; and  $\theta_{SE}$  is local sun elevation angle.

**Table 4** Results of land use comparison between 1987 and 2002 (ha)

1987	2002								
	Water	Irrigated	Outcrop	Meadow	Dry farming	Forest	Rangeland	Urban	Airport
Water	337.5	72.3	2.4	0	29.6	48.3	143.2	2.9	0
Irrigated	79.4	46,945.1	87.2	1217.4	20,446.6	406.1	18,603.6	1886.3	3.8
Outcrop	7.2	38.8	2881	2.7	1646.4	0	4971.7	4.2	0
Meadow	0	1746.2	7.3	6336.4	916.6	0	858.2	247.7	916.5
Dry farming	137.4	7140.4	123.8	246.4	71,143.4	6.3	14,907.4	831.2	62.4
Forest	0	757.7	0	40.8	582.9	1811.6	6863.5	1.9	0
Rangeland	123.9	12,250.5	1452.9	1810.2	61,205.5	400.9	164,613.8	1142.8	106.8
Urban	13.7	1042.3	2.5	34.5	649.9	0	1069.9	2510.9	43.6
Airport	0	0	0	0	0	0	0	0	0

Topographic normalization was performed because of extreme height differences in the study area. For this purpose, the Minnaert approach in Eq. 5 was used (ERDAS Imagine 9.2. Field Guide™, 2008):

$$BV_{normal\lambda} = \frac{BV_{observed\lambda} \cos e}{k(\cos i)(\cos e)} \tag{5}$$

where  $BV_{normal\lambda}$  is the normalized brightness value,  $BV_{observed\lambda}$  is the observed brightness value,  $i$  is the incident angle,  $e$  is the slope angle, and  $k$  is the empirically derived Minnaert constant.

**Object-based classification**

Object-based methods use information from texture, shape, and tone in addition to numerical values

(Bontemps et al. 2008; Dronova et al. 2011). The most evident difference between pixel-based and object-based image analysis is that, firstly, in object-based analysis, the basic processing units are image objects or segments, not single pixels. Secondly, the classifiers in object-based image analysis are soft classifiers that are based on fuzzy logic. Soft classifiers use membership to express an object’s assignment to a class. The membership value usually lies between 0.0 and 0.1, where 0.0 indicates absolute improbability assignment to a class and 1.0 indicates complete assignment to a class. The degree of membership depends on the degree to which the objects fulfill the class-describing condition. One advantage of such soft classifiers lies in the possibility of expressing uncertainties regarding the description of the classes (Bontemps et al. 2008; Dronova et al. 2011). Fuzzy classification is usually used in

**Table 5** Results of land use comparison between 2002 and 2013 (ha)

2002	2013								
	Water	Irrigated	Outcrop	Meadow	Dry farming	Forest	Rangeland	Urban	Airport
Water	535.1	8.8	1.5	9.9	42.4	4.4	50.8	46.4	0
Irrigated	58.2	41,775.7	202.2	213.4	16,832.3	380.6	8237.9	2217.4	67.2
Outcrop	2.9	60.3	3253.9	1.3	186.8	7.9	969.3	80.4	0
Meadow	1.9	485.2	5.6	5562.5	1833.9	0	931.4	762.9	104.1
Dry farming	184.3	14,067.1	179.8	367.2	119,476.4	8.4	25,299.7	3041.1	20.4
Forest	0.9	686.4	0	0	128.5	1253.7	583.8	0.9	8.4
Rangeland	167.3	22,065.8	317.1	267.8	69,005.5	1466.9	113,499.6	2453.1	36.4
Urban	4.2	380.7	13.4	77.3	1088.1	7.7	245.8	4435.4	73.9
Airport	0	16.1	23.3	23.4	45.1	0	117.1	45.2	859.3

**Table 6** Results of land use comparison between 1987 and 2013 (ha)

1987	2013								
	Water	Irrigated	Outcrop	Meadow	Dry farming	Forest	Rangeland	Urban	Airport
Water	410.2	69.3	4.7	0	29.7	48.1	72.4	2.9	0
Irrigated	212.4	47,825.4	238.8	801.7	21,015	348.1	15,778.6	3539.8	55.7
Outcrop	16.7	97.1	3461.2	3.6	2312.9	28.1	3867	66.5	0
Meadow	4.9	1281.8	26.8	5026.9	2047.3	0	616.6	1024.2	999.7
Dry farming	138.1	4650.6	293.3	170.3	84,780	0	8345.7	2271.9	0
Forest	0	2895.6	0	8.3	519.9	1940	4840.4	28.9	0
Rangeland	163.6	22,590.3	3088.6	504.8	97,156.6	894.7	116,930	3086.9	53.7
Urban	6.3	807.5	6.8	9.5	850.3	68.2	0	0	0
Airport	0	0	0	0	0	0	0	0	0

eCognition software, where it presents a type of nearest neighbor classification.

A segment is a group of adjacent pixels in an area in which likeness, such as number value or texture, is the most common criterion between them. Image

segmentation is very important in supplying the basic building blocks for object-based image analysis and the accuracy with which this phase is carried out influences the quality of the object-based classification. Segmentation can take into account factors such as shape, texture

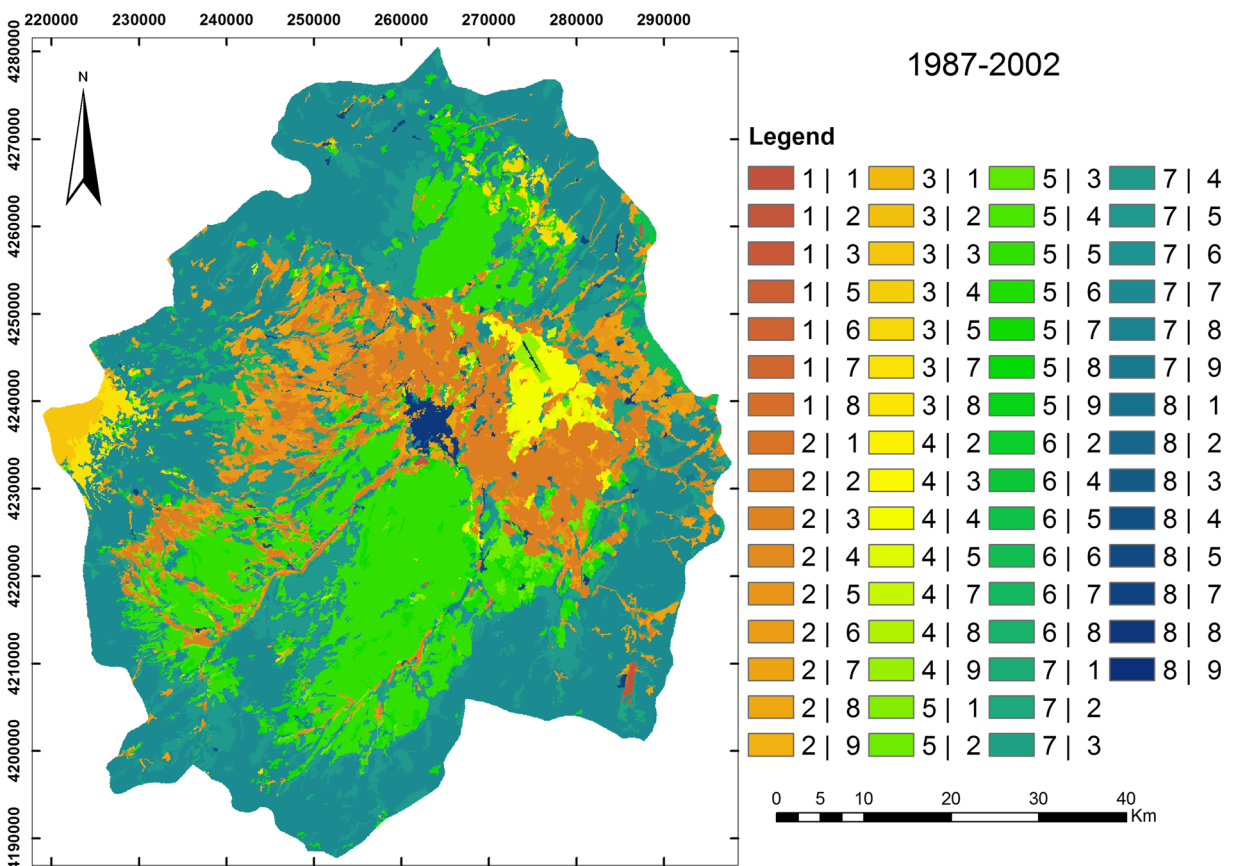


**Fig. 5** LULC change from 1987 to 2002. (The numbers in the legends correspond to the LULC classes, listed under the ID label in Table 3)



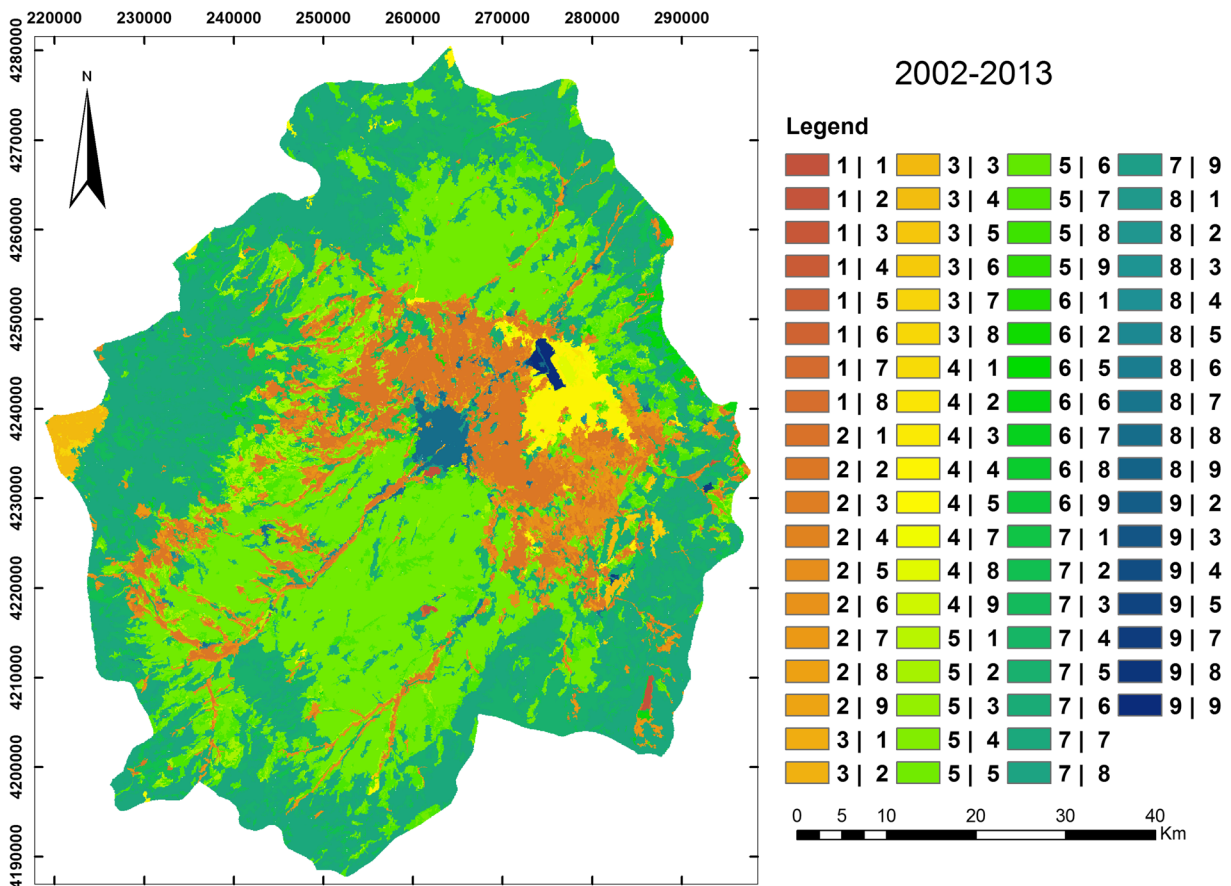


**Fig. 6** LULC change from 2002 to 2013. (The numbers in the legends correspond to the LULC classes, listed under the ID label in Table 3)

parameters, and the compactness coefficient (Zhang et al. 2005). Compactness parameter determines the segments density and the shape parameter is used for determination of softness/sharpness of the segments. Appropriate scale is another important factor for segmentation (Liu and Xia 2010). Different segmentations on an OLI image of part of the study area are presented in Fig. 3. Scale parameter determines size of the segments as shown in Fig. 3. The parameter values are selected based on “try and error” experimentally. This means we used different values for each and compare results until the best result is obtained. The object-based classification of images from 1987, 2002, and 2013 in this study makes use of different values of scale, compactness, and shape parameters for each image, in addition to the nearest neighbor algorithm. A comparison of segmentation and classification gave resulting values for the images equal to 20, 0.1, and 0.6 for 1987 image; 30, 0.1, and 0.5 for 2002 image; and 40, 0.6, and 0.5 for 2013 image, respectively for scale, compactness, and shape parameters.

### Accuracy assessment

A validation data set was used to assess the accuracy of each classification. There were 500 validation points taken from Google Earth for the map from 2013, 235 points for the map from 2002, and 170 points for the map from 1987 (100 points of those were initially collected by a Garmin Oregon 550 GPS, and then controlled using Google Earth imagery, because of the road accessibility limitation rest of the 400 points were collected only by Google Earth images). To overcome low-resolution problem of Landsat images by choosing ground control points (GCPs) based on some criteria (according to Campbell et al., 2015): (1) the sample unit must be  $\geq 90 \text{ m} \times 90 \text{ m}$  in size ( $3 \times 3$  Landsat pixels) (most units were significantly larger and then the collection was done at or near the center), (2) the entire area within the unit must be visually (and spectrally) homogeneous, and (3) the areas must have the maximum heterogeneous (variability) between units. Multivariate techniques were

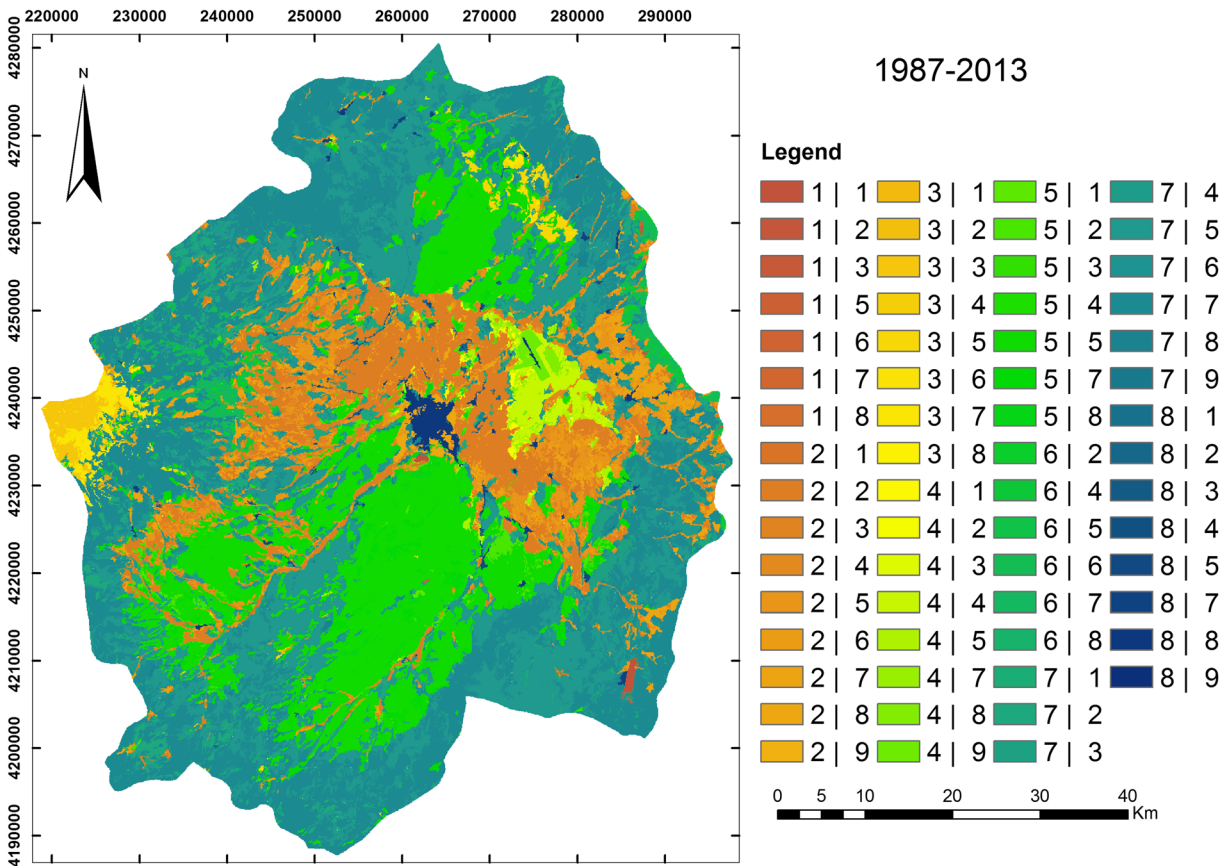


Fig. 7 LULC change from 1987 to 2013. (The numbers in the legends correspond to the LULC classes, listed under the ID label in Table 3)

used to perform the accuracy assessment, including an error matrix, overall accuracy, and a Kappa coefficient of agreement (Congalton and Green 2008) by class and overall classification. The error matrix was also used to calculate the producer’s accuracy, the user’s accuracy, and overall accuracy. The overall accuracy is defined as the proportion of pixels correctly classified divided by the total classified pixels, as shown in Eq. 6:

$$OA = \frac{\sum_{k=1}^N a_{kk}}{\sum_{i,k=1}^N a_{ik}} = \frac{1}{n} \sum_{k=1}^N a_{kk} \tag{6}$$

where N is the total number of pixels classified and  $\sum_{k=1}^N a_{kk}$  is the sum of the diagonal pixels. The producer’s accuracy relates to the probability that a reference sample was correctly mapped and measures the omission error (1—producer’s accuracy). In contrast, the user’s accuracy indicates the probability that a sample from the map actually matches the reference data and measures the commission error (1—user’s accuracy). As noted by

Foody (2004), the Kappa coefficient (formally estimated by  $\hat{K}$ ) is based on the comparison of predicted and actual class labels for each case in the validation data set, and is calculated using Eq. 7:

$$\hat{K} = \frac{p_0 - p_c}{1 - p_c} \tag{7}$$

where  $p_0$  is the proportion of cases in agreement and  $p_c$  is the proportion of agreement expected by chance.

LULC change detection over the selected time periods was analyzed using a post-classification comparison (PCC) technique with IDRISI Selva software and all information concerning LULC change was summarized.

### Results and discussion

The land-use maps from 1987, 2002, and 2013 derived from Landsat TM, ETM<sup>+</sup>, and OLI images can be seen in Fig. 4 and their overall accuracy and Kappa statistics

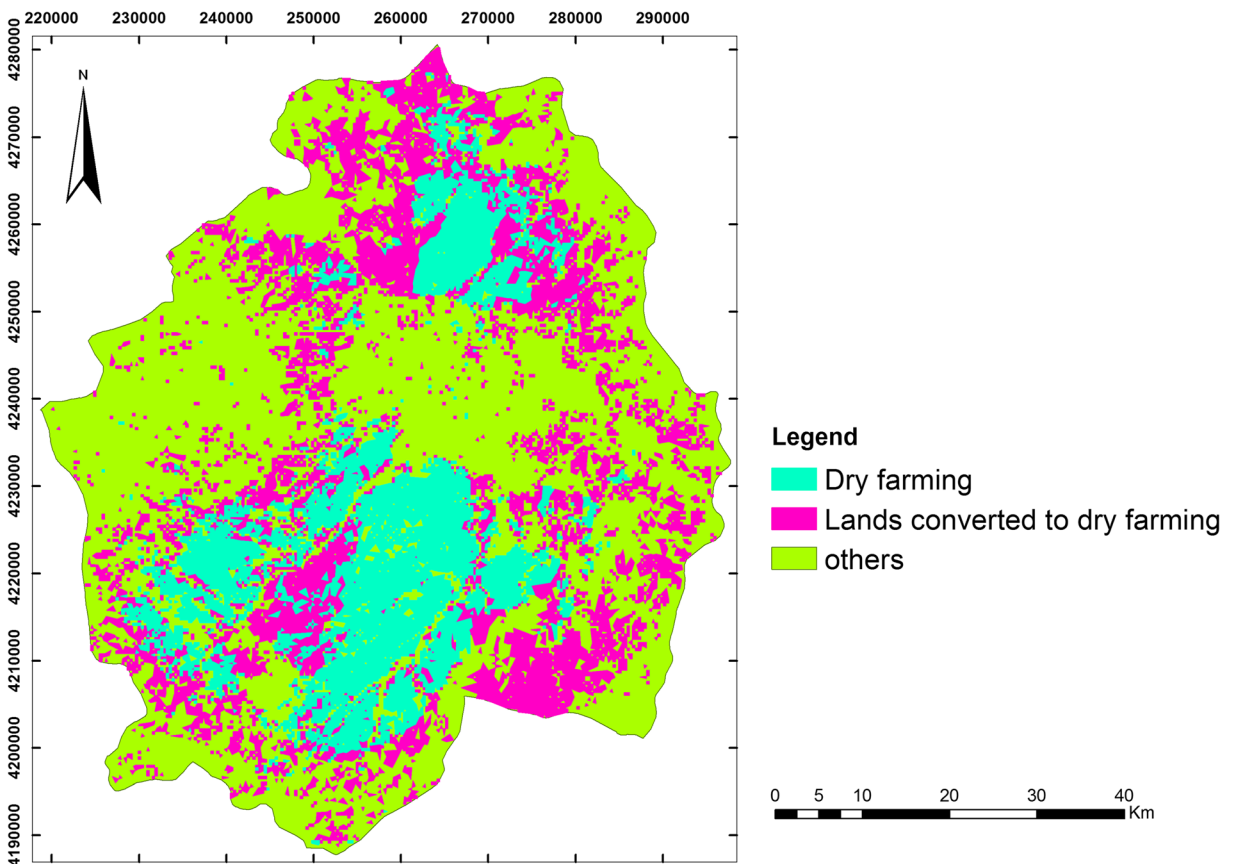


**Fig. 8** Land converted to dry farming from 1987 to 2013

in Table 2. The result of accuracy assessment shows high ability of object-based classification in producing LULC map.

Rangeland and dry farming are the predominant land uses in the study area for all 3 years, followed by irrigated farming. Forest cover appears relatively insignificant. As shown in Table 3, there has been considerable change in the study area from 1987 to 2013. Dry farming and urban areas have increased, while rangeland, forest, and meadow lands have decreased significantly. Irrigated farming area has decreased at first but has increased after 2002.

Measurements and locations of these changes are presented in Tables 4, 5, and 6, and Figs. 5, 6, and 7, respectively. Each label in Table 4 corresponds to a class in Fig. 6. The numbers in the legends of the figures correspond to the LULC classes, listed under the ID label in Table 3.

In addition, 97,156.6 ha of rangelands were converted to dry farming lands, constituting the most significant change in the study area, as shown in Fig. 8.

Medium-resolution satellite images such as Landsat images have been used for monitoring and mapping LULC from local to regional scales. Change detection and LULC mapping have increasingly been recognized as some of the most effective tools for urban and environmental resource management. Our results demonstrate the reliability and accuracy of using object-based remote sensing in LULC mapping and change detection in a heterogeneous region. The results of Aggarwal et al. (2016) and Petropoulos et al. (2012) have also demonstrated the high capacity of this method. Considering the appropriate accuracy assessment criteria and classification parameters using Landsat imagery and object-based classification, Cheţan et al. (2017) reported a range of 80 to 93% for overall accuracy using object-based classification and different variables. Moreover, the overall accuracy obtained by Olmanson and Bauer (2016) study ranges from 92.2 to 96.4% which even was improved using Lidar data (was peaked at 98%). The recent examples which are supporting our results show the high potential of object-based technique in similar classification and fields with

the lowest cost. Moreover, comparison of the results of previous studies, such as Azizi et al. (2016) and Mirzaei et al. (2018), which used pixel-based image analysis for LULC mapping and change detection in the Ardabil province, with the results of the present study, allows us to conclude that object-based image analysis has more advantages in this regard.

By considering LULC change from 1987 to 2013, the high amount of change in different land uses such as rangelands to dry farming lands is highlighted, indicating population increase, mismanagement, and inappropriate land policy in this region. Shalaby and Tateishi (2007), and Dewan and Yamaguchi (2009) have also reported the large changes in LULC associated with human development. This issue requires more attention from officials and rangeland managers for suitable land management. For example, assigning rangeland to agriculture goes contrary to the principles of sustainable development and can cause an increase in soil erosion and pest outbreaks, in turn causing soil and water pollution through the use of chemical fertilizers and pesticides. The effects of such land-use allocations are the focus of numerous studies, such as Hale et al. (2008). It is thus evident that past land policies and administration of these areas require in-depth scrutiny and review.

## Conclusion

In this study, medium resolution satellite Landsat images were classified using the object-based method, and LULC changes were detected through PCC. Validation of the classified maps indicates the high capacity of the object-based method. Change in different land uses, such as rangelands to dry farming lands, is considerable, showing links to human development, mismanagement, and inappropriate land policy in this area. In the north of the study area in 2013, rangelands have decreased considerably, having been converted to dry farming land. This issue requires more attention from officials and rangeland managers for suitable land management. If such trends of rangeland loss continue, effects such as soil erosion, especially on slopes, water and soil pollution, and pest outbreaks are predicted to increase considerably.

**Acknowledgements** We would like to thank Land Remote Sensing Program of the U.S. Geological Surveying collaboration with NASA for generously availing the Landsat 8 data.

## References

- Aggarwal, N., Srivastava, M., & Dutta, M. (2016). Comparative analysis of pixel-based and object-based classification of high resolution remote sensing images—a review. *International Journal of Engineering Trends and Technology*, 38, 5–11. <https://doi.org/10.14445/22315381/IJETT-V38P202>.
- Akbari, M., Mamanpoush, A. R., Gieske, A., Miranzadeh, M., Torabi, M., & Salmi, H. R. (2007). Crop and land cover classification in Iran using Landsat 7 imagery. *International Journal of Remote Sensing*, 27, 4117–4135. <https://doi.org/10.1080/01431160600784192>.
- Al Fugara, A. M., Pradhan, B., & Mohamed, T. A. (2009). Improvement of land-use classification using object-oriented and fuzzy logic approach. *Applied Geomatics*, 1, 111–120. <https://doi.org/10.1007/s12518-009-0011-3>.
- Amalisana, B., Rokhmatullah, X., & Hernina, R. (2017). Land cover analysis by using pixel-based and object-based image classification method in Bogor. *IOP Conf. Series: Earth and Environmental Science*. <https://doi.org/10.1088/1755-1315/98/1/012005>.
- Amini Parsa, V., & Salehi, E. (2016). Spatio-temporal analysis and simulation pattern of land use/cover changes, case study: Naghadeh, Iran. *Journal of Urban Management*, 5, 43–51. <https://doi.org/10.1016/j.jum.2016.11.001>.
- Aslami, F., Ghorbani, A., Sobhani, B., & Panahandeh, M. (2015). Comparing artificial neural network, support vector machine and object-based methods in preparation land use/cover maps using Landsat-8 images. *Iranian Journal of Remote Sensing and GIS Techniques in Natural Resources*, 6(3), 1–14 (In Persian).
- Azizi, A., Malakmohamadi, B., & Jafari, H. R. (2016). Land use and land cover spatiotemporal dynamic pattern and predicting changes using integrated CA-Markov model. *Global Journal of Environmental Science and Management*. <https://doi.org/10.7508/gjesm.2016.03.002>.
- Blaschke, T. (2010). Object based image analysis for remote sensing. *ISPRS Journal of Photogrammetry and Remote Sensing*, 65, 2–16. <https://doi.org/10.1016/j.isprsjrs.2009.06.004>.
- Bontemps, S., Bogaert, P., Titeux, N., & Defourmy, P. (2008). An object-based change detection method accounting for temporal dependencies in time series with medium to coarse spatial resolution. *Remote Sensing of Environmental*, 112, 3181–3191. <https://doi.org/10.1016/j.rse.2008.03.013>.
- Butt, A., Shabbir, R., Ahmad, S. S., & Aziz, N. (2015). Land use change mapping and analysis using remote sensing and GIS: a case study of Simly Watershed, Islamabad, Pakistan. *Egyptian Journal of Remote Sensing and Space Science*, 18, 251–259. <https://doi.org/10.1016/j.ejrs.2015.07.003>.
- Campbell, M., Congalton, R. G., Hartter, J., & Ducey, M. (2015). Optimal land cover mapping and change analysis in north-eastern Oregon using Landsat imagery. *Photogrammetric Engineering and Remote Sensing*, 81, 37–47. <https://doi.org/10.14358/PERS.81.1.37>.
- Chander, G., & Markham, B. L. (2003). Revised Landsat-5 TM radiometric calibration procedures, and post-calibration dynamic ranges. *IEEE Journal of Transactions on Geoscience and Remote Sensing*, 41, 2674–2677. <https://doi.org/10.1109/TGRS.2003.818464>.



- Chetan, M. A., Dornik, A., & Urdea, P. (2017). Comparison of object and pixel-based land cover classification through three supervised methods. *Journal of Geodasy, Geoinformation and Land Management*. <https://doi.org/10.12902/zfv-0165-2017>.
- Congalton, R. G., & Green, K. (2008). *Assessing the accuracy of remotely sensed data: principles and practices*. Boca Raton, FL: CRC Press.
- Coppin, P., Jonckheere, I., Nackaerts, K., Muys, B., & Lambin, E. (2004). Digital change detection methods in ecosystem monitoring: a review. *International Journal of Remote Sensing*, 25, 1565–1596. <https://doi.org/10.1080/0143116031000101675>.
- Dewan, A. M., & Yamaguchi, Y. (2009). Land use and land cover change in Greater Dhaka, Bangladesh: using remote sensing to promote sustainable urbanization. *Journal of Applied Geography*, 29, 390–401. <https://doi.org/10.1016/j.apgeog.2008.12.005>.
- Dronova, I., Gong, P., & Wang, L. (2011). Object-based analysis and change detection of major wetland cover types and their classification uncertainty during the low water period at Poyang Lake, China. *Remote Sensing of Environment*, 115, 3220–3236. <https://doi.org/10.1016/j.rse.2011.07.006>.
- Du, Y., Wu, D., Liang, F., & Li, C. (2013). Integration of case-based reasoning and object-based image classification to classify SPOT images: a case study of aquaculture land use mapping in coastal areas of Guangdong Province, China. *GIScience and Remote Sensing Journal*. <https://doi.org/10.1080/15481603.2013.842292>.
- El-Asmar, H. M., Hereher, M. E., & El-Kafrawy, S. B. (2013). Surface area change detection of the Burullus Lagoon, North of Nile delta, Egypt, using water indices: a remote sensing approach. *Egyptian Journal of Remote Sensing and Space Science*, 16, 119–123. <https://doi.org/10.1016/j.ejrs.2013.04.004>.
- Enderle, D. I. M., & Weih, Jr, R. C. (2005). Integrating supervised and unsupervised classification methods to develop a more accurate land cover classification. *Journal of the Arkansas Academy of Science*, <http://scholarworks.uark.edu/jaas/vol59/iss1/10>
- Erbek, F. S., Ozkan, C., & Taberner, M. (2004). Comparison of maximum likelihood classification method with supervised artificial neural network algorithms for land use activities. *International Journal of Remote Sensing*, 25, 1733–1748. <https://doi.org/10.1080/0143116031000150077>.
- ERDAS Imagine 9.2. *Field Guide™*. 2008. Leica Geosystems GIS and Mapping LLC.
- Foody, G. M. (2004). Thematic map comparison: evaluating statistical significance of differences in classification accuracy. *Photogrammetric Engineering and Remote Sensing*, 70, 627–633. <https://doi.org/10.14358/PERS.70.5.627>.
- Gao, Y., & Mas, J. F. (2008). A comparison of the performance of pixel based and object based classifications over images with various spatial resolutions. *Online Journal of Earth Sciences*, <http://medwelljournals.com/abstract/?doi=ojesci.2008.27.35>
- Ghebregabher, M. G., Yang, T., Yang, X., Wang, X., & Khan, M. (2016). Extracting and analyzing forest and woodland cover change in Eritrea based on Landsat data using supervised classification. *Egyptian Journal of Remote Sensing and Space Science*. <https://doi.org/10.1016/j.ejrs.2015.09.002>.
- Ghorbani, A., Kakemami, A., & Kavianpour, H. (2011). Change detection of urban areas in Ardabil Province during the last 5 decades using aerial photography and Landsat images. 23<sup>rd</sup> *Asian Conference on Remote Sensing*, Tapei, Taiwan, 3-7 October. Volume 2 of 4.
- Ghorbani, A., Mohammadi Moghaddam, S., Hashemi Majd, K., & Dadgar, D. (2018). Spatial variation analysis of soil properties using spatial statistics: a case study in the region of Sabalan Mountain, Iran. *Journal on Protected Mountain Areas Research*, 1, 70–80. <https://doi.org/10.1553/eco.mont-10-1s70>.
- Griffiths, P., Hoster, P., Grubner, O., & van der Linden, S. (2010). Mapping megacity growth with multi sensor data. *Remote Sensing of Environment*, 114, 426–439. <https://doi.org/10.1016/j.rse.2009.09.012>.
- Hale, R. C., Gallo, K. P., & Loveland, T. R. (2008). Influences of specific land use/land cover conversions on climatological normals of near-surface temperature. *Journal of Geophysical Research*, 113. <https://doi.org/10.1029/2007JD009548>.
- Halimi, M., Sedighifar, Z., & Mohammadi, C. (2017). Analyzing spatiotemporal land use/cover dynamic using remote sensing imagery and GIS techniques case: Kan Basin of Iran. *GeoJournal*. <https://doi.org/10.1007/s10708-017-9819-2>.
- Hussain, E., & Shan, J. (2015). Object-based urban land cover classification using rule inheritance over very high-resolution multisensory and multi-temporal data. *GIScience and Remote Sensing*, 53, 164–182. <https://doi.org/10.1080/15481603.2015.1122923>.
- Im, J., Jensen, J. R., & Hodgson, M. E. (2013). Object-based land cover classification using high-posting-density LiDAR data. *GIScience and Remote Sensing*, 45, 209–228. <https://doi.org/10.2747/1548-1603.45.2.209>.
- Jawak, S. D., Devliyali, P., & Luis, A. (2015). A comprehensive review on pixel oriented and object oriented methods for information extraction from remotely sensed satellite images with a special emphasis on cryospheric applications. *Advances in Remote Sensing*, 04, 177–195. <https://doi.org/10.4236/ars.2015.43015>.
- Jayanth, J., Kumar, A. T., Koliwad, S., & Krishnashastry, S. (2016). Identification of land cover changes in the coastal area of Dakshina Kannada District, South India during the year 2004–2008. *Egyptian Journal of Remote Sensing and Space Science*. <https://doi.org/10.1016/j.ejrs.2015.09.001>.
- Lewinski, S. (2006). Object-oriented classification of Landsat ETM+ satellite image. *Journal of Water and Land Development*, 10. <https://doi.org/10.2478/v10025-007-0008-4>.
- Li, Q., Wang, C., Zhang, B., & Lu, L. (2015). Object-based crop classification with Landsat-MODIS enhanced time-series data. *Remote Sensing*, 7, 16091–16107. <https://doi.org/10.3390/rs71215820>.
- Lillesand, T. M., Kiefer, R. W., & Chipman, J. W. (2008). *Remote sensing and image interpretation*. Hoboken, NJ: John Wiley and Sons, Inc..
- Liu, D., & Xia, F. (2010). Assessing object-based classification: advantages and limitation. *Remote Sensing Letters*, 1, 187–194. <https://doi.org/10.1080/01431161003743173>.
- Long, J. A., Lawrence, R. L., Greenwood, M. C., Marshall, L., & Miller, P. R. (2013). Object-oriented crop classification using multitemporal ETM+ SLC-off imagery and random forest. *GIScience and Remote Sensing*. <https://doi.org/10.1080/15481603.2013.817150>.
- Lu, D., Mausel, P., Brondizio, E., & Moran, E. (2004). Change detection techniques. *International Journal of*

- Remote Sensing*, 25, 2365–2401. <https://doi.org/10.1080/0143116031000139863>.
- Mirzaei Mossivand, A., Ghorbani, A., & Keivan Behjou, F. (2018). Land use/cover change detection using Landsat and IRS imagery: a case study, Khalkhal County. *Iranian Journal of Geographic Space*, 60, 101–116 (In Persian).
- Myint, S. W., Gober, P., Brazel, A., Grossman-Clarke, S., & Weng, Q. (2011). Per-pixel vs. object-based classification of urban land cover extraction using high spatial resolution imagery. *Remote Sensing of Environment*, 115, 1145–1161. <https://doi.org/10.1016/j.rse.2010.12.017>.
- Olmanson, L. G., & Bauer, M. E. (2016). Improved land cover classification by integrating Landsat imagery with Lidar and object-based image analysis for land cover classification of the international lake of the woods/rainy river basin. [http://lps16.esa.int/posterfiles/paper2097/Landcover\\_poster32\\_40\\_final.pdf](http://lps16.esa.int/posterfiles/paper2097/Landcover_poster32_40_final.pdf)
- Petropoulos, G. P., Kalaitzidis, C., & Vadrevu, K. P. (2012). Support Vector Machines and object-based classification for obtaining land-use/cover cartography from Hyperion hyperspectral imagery. *Computers and Geosciences*, 41, 99–107. <https://doi.org/10.1016/j.cageo.2011.08.019>.
- Phinn, S., Stanford, M., Scarth, P., Murry, A. T., & Shyy, P. T. (2002). Monitoring the composition of urban environment based on the vegetation-impervious surface-soil (VIS) model by subpixel analysis techniques. *International Journal of Remote Sensing*, 23, 4131–4153. <https://doi.org/10.1080/01431160110114998>.
- Phiri, D., & Mogenroth, J. (2017). Developments in Landsat land cover classification methods: a review. *Remote Sensing*, 9. <https://doi.org/10.3390/rs9090967>.
- Rawat, J. S., & Kumar, M. (2015). Monitoring land use/cover change using remote sensing and GIS techniques: a case study of Hawalbagh Block, District Almora, Uttarakhand, India. *Egyptian Journal of Remote Sensing and Space Science*, 18, 77–84. <https://doi.org/10.1016/j.ejrs.2015.02.002>.
- Reed, B. C., White, M., & Brown, J. F. (2003). *Remote sensing phenology*. In M. D. Schwartz (Ed.), *Phenology: an integrative environmental science* (pp. 365–381). Dordrecht: Kluwer Academic Publishers.
- Roostaie, S., Alavi, S. A., Nikjoo, M. R., & Valizade Kamran, K. (2012). Evaluation of object-oriented and pixel based classification methods for extracting changes in urban area. *International Journal of Geomatics and Geosciences*, 2(3), 738–749.
- Shalaby, A., & Tateishi, R. (2007). Remote sensing and GIS for mapping and monitoring land cover and land use changes in the northwestern coastal zone of Egypt. *Applied Geography*, 27, 28–41. <https://doi.org/10.1016/j.apgeog.2006.09.004>.
- Sharifi, J., Fayaz, M., Azimi, F., Rostami Kia, Y., & Eshvari, P. (2013). *Identification of ecological region of Iran (vegetation of Ardabil Province)*. Institute Research of Forest and Rangeland Press, Report No. 42183/37. (In Persian).
- Sinha, S., Sharma, L. K., & Nathawat, M. S. (2015). Improved land-use/land cover classification of semi-arid deciduous forest landscape using thermal remote sensing. *Egyptian Journal of Remote Sensing and Space Science*. <https://doi.org/10.1016/j.ejrs.2015.09.005>.
- Solaimani, K., Arekhi, M., Tamartash, R., & Miryaghobzadeh, M. (2010). Land use/cover change detection based on remote sensing data (a case study: Neka Basin). *Agriculture and Biology Journal of North America*, 1, 1148–1157. <https://doi.org/10.5251/abjna.2010.1.6.1148.1157>.
- Taati, A., Sarmadian, F., Mousavi, A., Hossein Pour, C. T., & Shahir, A. H. E. (2015). Land use classification using support vector machine and maximum likelihood algorithms by Landsat 5 TM images. *Walailak Journal of Science and Technology*. <https://doi.org/10.14456/WJST.2015.33>.
- Teimoorzadeh, A., Ghorbani, A., & Kavianpoor, A. H. (2015). Study on the flora, life forms and chorology of the south eastern of Namin forests (Asi-Gheran, Fandoghloo, Hasani and Bobini). *Ardabil Province. Iranian Journal of Plant Biology*, 28(2), 264–275 (In Persian).
- Weih, R. C., & Riggan, N. D. (2010). Object-based classification vs. pixel-based classification: comparative importance of multi-resolution imagery. *The International Archives of the Photogrammetry, Remote Sensing and Spatial Information Sciences*, Vol. XXXVIII-4/C7.
- Wells, W. K. (2010). *Object-based segmentation and classification of one meter imagery for use in forest management plans*. MSc Diss: University of Utah <http://digitalcommons.usu.edu/etd/653>.
- Whiteside, T. G., Boggs, G. S., & Maier, S. W. (2011). Comparing object-based and pixel-based classification for mapping savannas. *International Journal of Applied Earth Observation and Geoinformation*, 13, 884–893. <https://doi.org/10.1016/j.jag.2011.06.008>.
- Wulder, M. A., White, J. C., & Coops, N. C. (2006). *Identifying and describing forest disturbance and spatial pattern: data selection issues and methodological implications*. In M. A. Wulder & S. E. Franklin Boca Raton (Eds.), *Understanding forest disturbance and spatial pattern: remote sensing and GIS approaches* (pp. 31–61). FL: CRC Press Taylor and Francis Group.
- Zhang, B., Song, M., & Zhou, W. (2005). Exploration on method of auto-classification for main ground objects of three gorges reservoir area. *Chinese Geographical Science*, 15, 157–161. <https://doi.org/10.1007/s11769-005-0009-7>.